Electronic Supplementary Material (ESI) for Chemical Science.

Feasible Bottom-up Development of Conjugated Microporous Polymers (CMPs) for Boosting the Deep Removal of Sulfur Dioxide

He Li,[a] Hanqian Pan,[b] Yijian Li,[b] ShuaiShuai Shang,[a] Shihui Huang,[a] Xili Cui,*[b] Jun Hu,*[a] Honglai Liu[a]

Abstract: A pain-point for material development is that computer-screened structures are usually difficult to be realized in experiments. Herein, considering linkages are crucial for building functional nanoporous polymers with diverse functionalities, we develop an efficient approach for constructing target-specific conjugated microporous polymers (CMPs) based on screening the feasible polymerization pathways. Taking the deep removal of SO_2 from the SO_2/CO_2 mixture as the specific target, we precisely screen the linkages and fabricate different CMPs by manipulating the porosity and hydrophobicity. Based on the optimized Buchwald-Hartwig amination, the obtained CMPs can achieve the SO_2/CO_2 selectivity as high as 113, and the moderate Q_{st} of 30 kJ mol^{-1} for feasible regeneration. Furthermore, the potential of CMPs for practical SO_2/CO_2 separation is demonstrated through continued breakthrough tests. The SO_2 binding sites are consistent with the screening results and proved by in-situ Fourier Transform Infrared spectroscopy and Grand Canonical Monte Carlo simulation, providing solid feasibility for the synthesis realizability for future boosts of task-specific CMPs.

Table of Contents

Section 1. Simulation models

The density functional theory (DFT) calculations were carried out using a Gaussian 09 Package.[31] The ground state conformations of SO_2, CO_2 and all the CMPs segments were optimized using opt/rb3lyp/6-311g (d, p) method. The binding energies (BEs) were calculated through the equation 1.

$$E = E_{total} - E_{fragment} - E_{molecule} \quad \text{(Eq. 1)}$$

Simulated polymerization algorithm was performed through Dendrimer and Amorphous Cell package in Materials Studio[32] to generate initial structure of TMM-PD, TMM-BD, TMM-TFPD and TMM-DMDF, with the density of 0.3 cm^3g^{-1}. All CMPs cells were contained 400 Argon atoms to prevent the stacking of the polymer chain. Then, to approximate the experimental value and remove the local non-equilibrium, several energy minimization and dynamic steps were performed. First, argon molecules were removed from the 3D models in three stages and, after each removal, cycles of energy minimization and NVT dynamics (the canonical NVT ensemble is characterized by constant number of molecules N, volume V and temperature T) were conducted in accordance with the downscaling procedure. The models were then subjected to compression at temperatures of 300 K through NPT-MD runs to obtain the initial density similar to the experimental one. The cells were equilibrated by performing NVT dynamics (T=600 K for 50 ps, T=300 K for 20 ps) and then NPT dynamics at very low pressure (P=0.1 bar for 20 ps) to prevent the increase of systems energy. The final equilibration was carried out by an MD simulation of 500 ps (NPT, P=1 bar), having verified that this time is sufficient to allow the system to reach an almost constant value of total energy. Furthermore, the simulated adsorption isotherms were performed by Sorption package through grand canonical Monte Carlo (GCMC) method, in which the sorption method, forcefield and charges were used as Metropolis, COMPASS27, Forcefield assigned, respectively. The electrostatic interaction was calculated by the Ewald summation method with an accuracy 1 x 10^{-5} kcal/mol. The long ranges tail of the Lennard–Jones (LJ) potential is truncated at 12.5 Å, where the discontinuity of the interacting potential at the truncation point is smoothed by the cubic spline method with a spline width 1 Å and a buffer width 0.5 Å.

Section 2. Synthesis and Characterization methods

2.1 Materials

Tetra(4-bromophenyl)methane (TMM, 98%) was purchased from Shanghai Tensus Biotech Co.,LTD. Tetrafluorophenylenediamine (PD, 99%), 2, 4-tetrafluorophenylenediamine (TFPD, 99%), 4, 4 '-diaminobiphenyl (BD, 98%) and 2,2' -difluoro-4, 4 '-diaminobiphenyl (DMDF, 95%) Benzimidazole (BzIM, 98%) and 2-aminobenzimidazole (2-amBzIM, 97%) were purchased J&K scientific. 1, 4-phenylboric acid (BA), 1, 3, 5-tritynyl benzene and p-phenyldibromine were purchased from Tokyo Chemical Industry. Ultra-dry N, N-dimethylformamide (DMF, 99.5%, Super Dry), and ultra-dry tetrahydrofuran (THF, 99.5%, Super Dry) were purchased from Shanghai 3A Chemical Technology Co., LTD. The catalysts of tetratriphenylphosphone-palladium, cuprous iodide, bis (dibenzylidenone) palladium ($Pd(dba)_2$, 63.9-78.1% carbon loaded, 16.6-20.4% Palladium loaded) and 2-dicyclohexylphosphone-2', 4', 6' -triisopropyl biphenyl (XPhos, 97%) were purchased from Suzhou Xinjiayuan Chemical Technology Co., LTD. Sodium tert-butanol (NaOtBu) and sodium chloride (NaCl) were purchased from Shanghai Titan Technology Co., LTD. All materials are used directly without further purification.

2.2 Synthesis Procedures

TMM-PD, TMM-BD, TMM-TFPD

100 mL of Schlenk tube was subjected to strict dehydrating and deoxygenating operation, followed by adding 0.159g TMM, 0.052g PD or 0.09g TFPD, 0.092g BD and 0.0143g XPhos respectively under the protection of argon gas. After vacuum treatment for three times, 0.0115 g $Pd(dba)_2$, 0.028 g NaCl and 0.221 g sodium tert-butanol were flushed into argon and then 15 mL ultra-dry THF was added and reacted at 85 ^oC for 48 h. After the reaction was cooled to room temperature, 200 mL THF, 80 ^oC hot water, methanol and chloroform were used for extraction and leaching for three times to remove excess catalysts and oligomers. Then, the prepared CMPs were deeply washed by Soxhlet extraction of THF, methanol and chloroform for 24 h, and the resulting products were dried under vacuum at 80 ^oC.

TMM-BA

TMM-BA was prepared by typical Suzuki-Miyaura cross-coupling.[1] For the synthesis of TMM-BA, 0.1208g TMM and 0.063g BA were added into a three-mouth flask and dispose with three times of degassing and pump into argon. Then ultra-dry DMF and 2 mL of K_2CO_3 solution were added for further half an hour of degassing. Finally, the catalyst tetratriphenylphosphine palladium was added under the protection of argon gas and reacted at 150 ^oC for 36 h. The obtained polymer was extracted in methanol, dichloromethane, toluene and tetrahydrofuran by Soxhlet extraction.

CMP-1 was synthesized according to the previous work.[2]

2.3 Characterization

Fourier transform infrared spectroscopy (FTIR) was employed by using a NEXUS 470 (Thermo Nicolet) with a scan range from 400 to 4000 cm^{-1}. XPS spectra were analyzed by ESCALAB 250Xi (Thermo Fisher Co.) with resolution greater than 3 um. The powder crystal structure of TMM-PD and TMM-BD were analyzed by Rotating Anode X-ray Powder Diffractometer, 18KW/D/max2550VB/PC (Copper Target 18KW(450mA), Programmed Variable Slit System, Fully Automated Curved (Plate) Crystal Graphite Monochoromator, JADE 5.0Software, Anton Paar XRK-900 High Temperature in-situ Reactor, the rage of 2θ=5°-35°, at a step of 0.02°). The morphology of all CMPs were analyzed with a field emission scanning electron microscope (FESEM), S-3400N (HITACHIJapan) and high resultion transmission electron microscopy (TEM), JEM-2100 (Japan). The surface area, N_2 adsorption (liquid nitrogen bath) of all CMPs were all collected on Micrometrics tristar II. Each sample was degassed for 8 h at 373K before analysis. The adsorption-desorption isotherms of SO_2 and CO_2 were analyzed by BSD-VVS (BEISHIDE Instrument Co.), each sample was degassed for 2 h at 353K before analysis.

2.4 Fitting of SO_2, CO_2, and H_2O adsorption isotherm[3-5]

The adsorption isottherm of SO_2 and CO_2 were fitted with the dual-site Langmuir-Freundlich model (equation 2). The parameters are summarized in Table S1.

$$q = q_{A,\,sat}\frac{ap^k}{1+ap^k} + q_{B,sat}\frac{bp^y}{1+bp^y} \quad \text{(Eq. 2)}$$

where p is the pressure of the bulk gas at equilibrium with the adsorbed phase (kPa), q is the adsorbed amount per mass of adsorbent (mol kg^{-1}), $q_{A,sat}$ an $q_{B,sat}$ are the saturation capacities of site A and B (mmol g^{-1}), a and b are the affinity coefficients (kPa^{-1}), k and y represented the deviations from an ideal homogeneous surface.

2.5 IAST selectivity calculation

The selectivities for SO_2/CO_2 separation were calculated using the equation 3.

$$S = \frac{q_1/q_2}{p_1/p_2} \quad \text{(Eq. 3)}$$

where q_1 and q_2 are the molar loadings in the adsorbed phase in equilibrium with the bulk gas phase with partial pressures p_1 and p_2.

2.6 Adsorption heat (Q_{st})

A virial-type expression comprising the temperature-independent parameters a_i and b_j was employed to calculate the heat of adsorption for SO_2 and CO_2. In each case, the data were fitted using the equation:

$$\ln P = \ln N + \left(\frac{1}{T}\right)\sum_{i=0}^{m} a_i N^i + \sum_{j=o}^{n} b_j N^j \quad \text{(Eq.4)}$$

Where P is the pressure expressed in kPa, N is the amount adsorbed in mmol g^{-1}, T is the temperature in K, a_i and b_j are virial coefficients, m and n represent the number of coefficients required to describe the isotherms adequately.

The adsorption enthalpy was calculated through virial coefficients.

$$Q_{st} = -R\sum_{i=0}^{m} a_i N^i \quad \text{(Eq.5)}$$

2.7 Breakthrough test

All breakthrough tests were performed in dynamic gas breakthrough equipment and conducted using a stainless-steel column (4.6 mm inner diameter × 50 mm) manually packed with CMPs. The column was first purged with He flow (10 mL min^{-1}) for 24 h at 353 K. The mixed gas of SO_2/CO_2 (0.2%/99.8%, v/v) was then introduced at 20 mL min^{-1}. Outlet gas from the column was continuously monitored using gas chromatography (GC-2010 plus, SHIMADZU) with a thermal conductivity detector (TCD) coupled with a flame ionization detector (FID).

Section 3. Supporting Figures

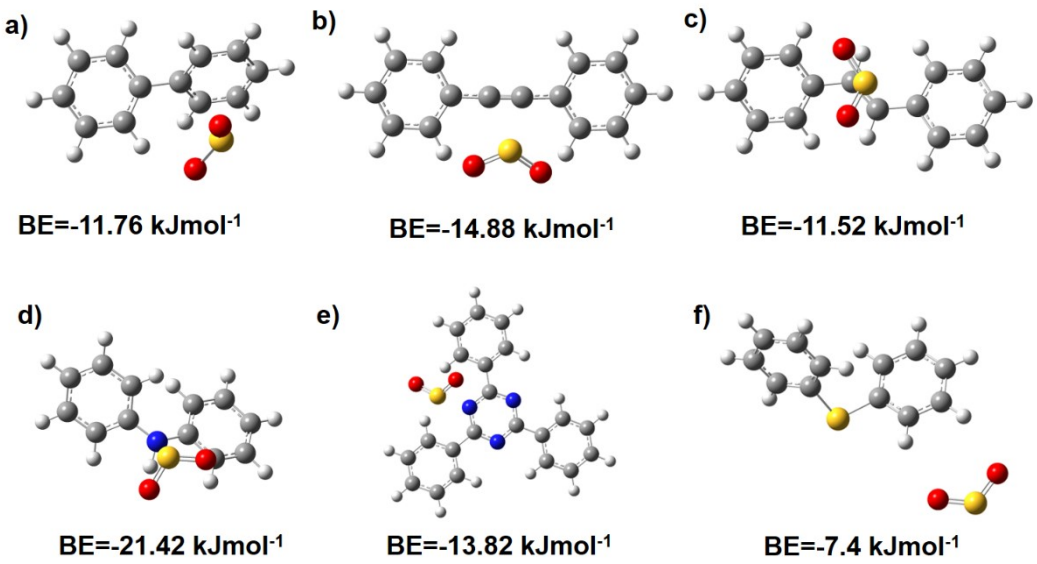

Figure S1. BEs between a) Suzuki-Miyaura cross-coupling; b) Sonogashira-Haglihara cross-coupling; c) Heck reaction; d) Buchwald-Hartwig amination; e) Cyclotrimerization; f) Thioether connection with SO_2 molecule.

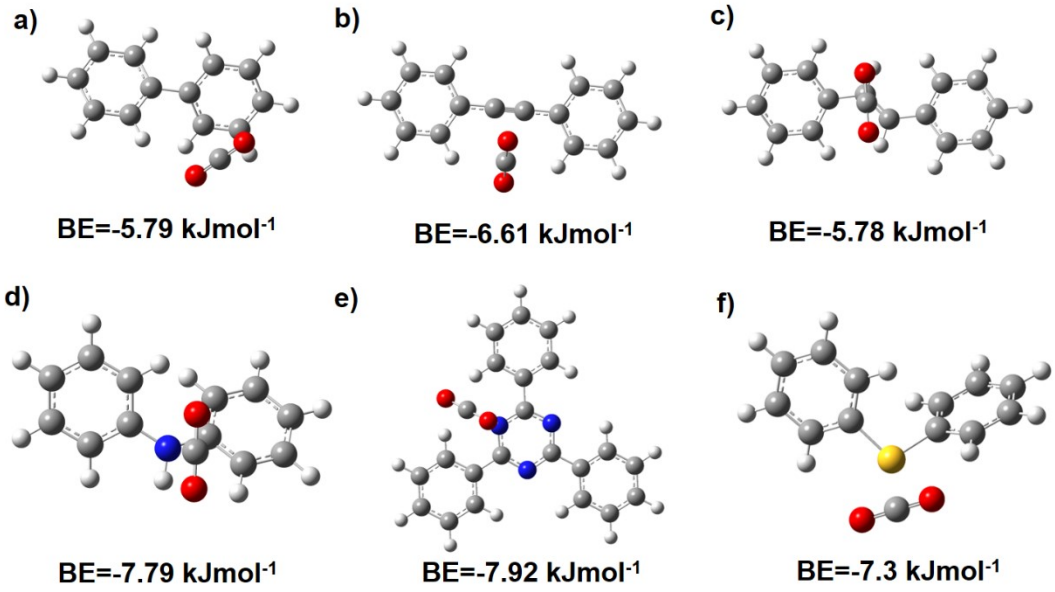

Figure S2. BEs between a) Suzuki-Miyaura cross-coupling; b) Sonogashira-Haglihara cross-coupling; c) Heck reaction; d) Buchwald-Hartwig amination; e) Cyclotrimerization; f) Thioether connection with CO_2 molecule.

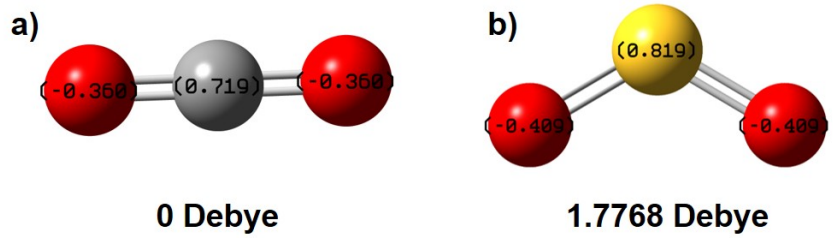

Figure S3. Polarity and electrostatic distribution of a) CO_2 and b) SO_2.

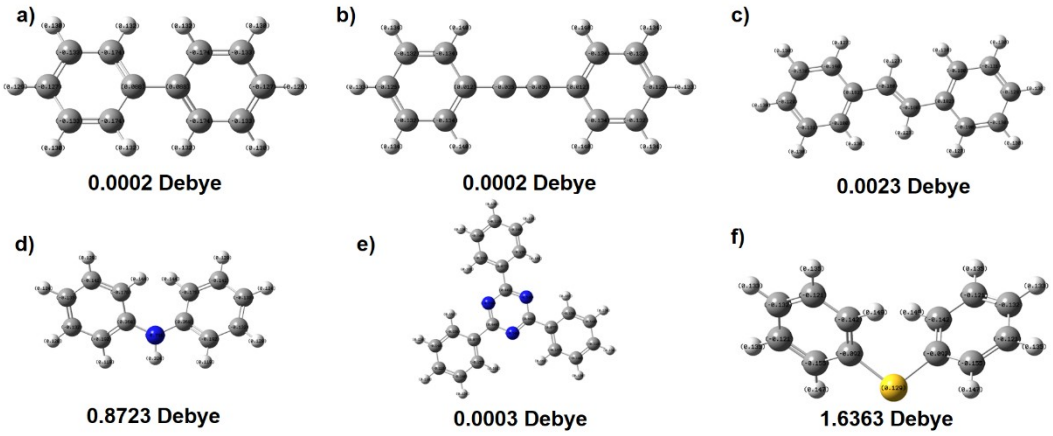

Figure S4. Polarity and electrostatic distribution of a) Suzuki-Miyaura cross-coupling; b) Sonogashira-Haglihara cross-coupling; c) Heck reaction; d) Buchwald-Hartwig amination; e) Cyclotrimerization; f) Thioether connection.

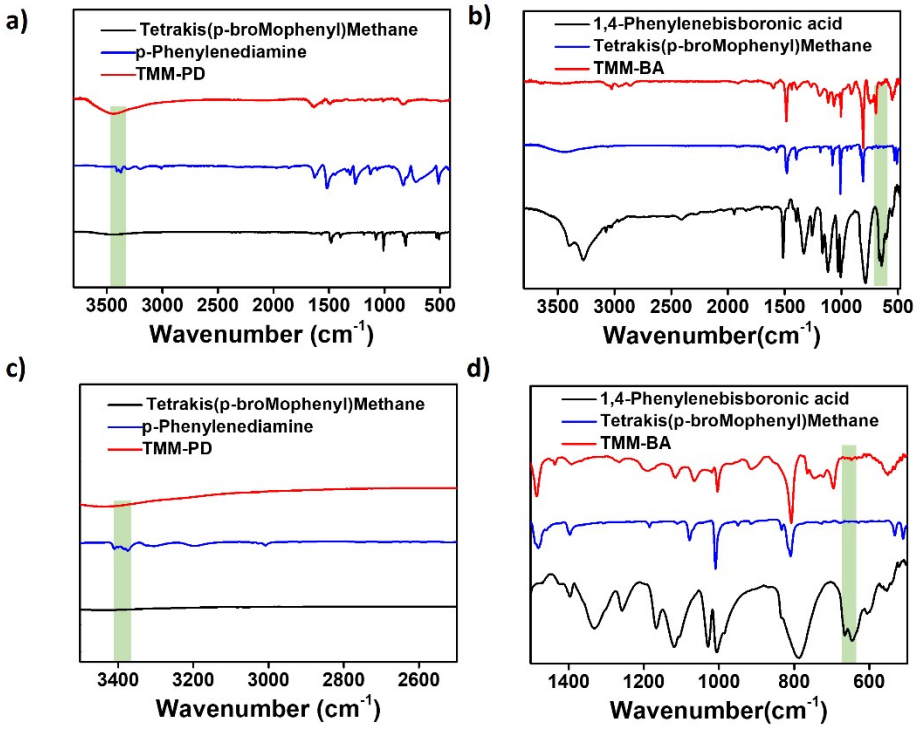

Figure S5. FTIR contrastive spectra of monomers and polymers: a) TMM-PD and b) TMM-BA. Enlarged FTIR contrastive spectra of monomers and

polymers: c) TMM-PD and d) TMM-BA.

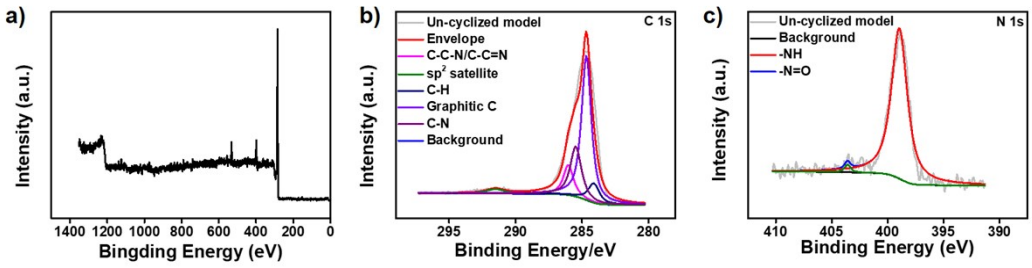

Figure S6. XPS spectra of TMM-PD.

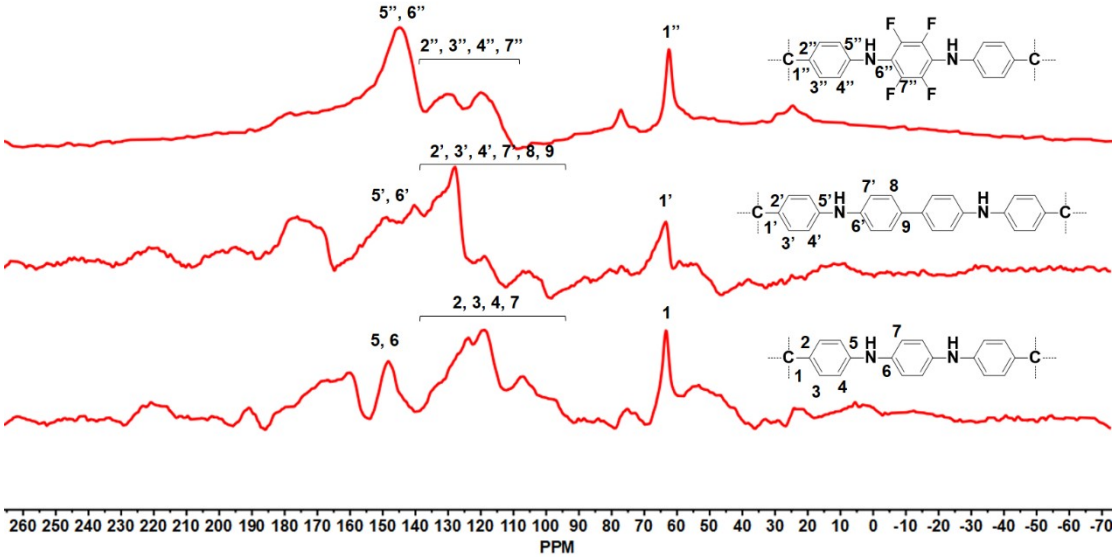

Figure S7. Solid-state NMR spectra of TMM-PD, TMM-BD, and TMM-TFPD.

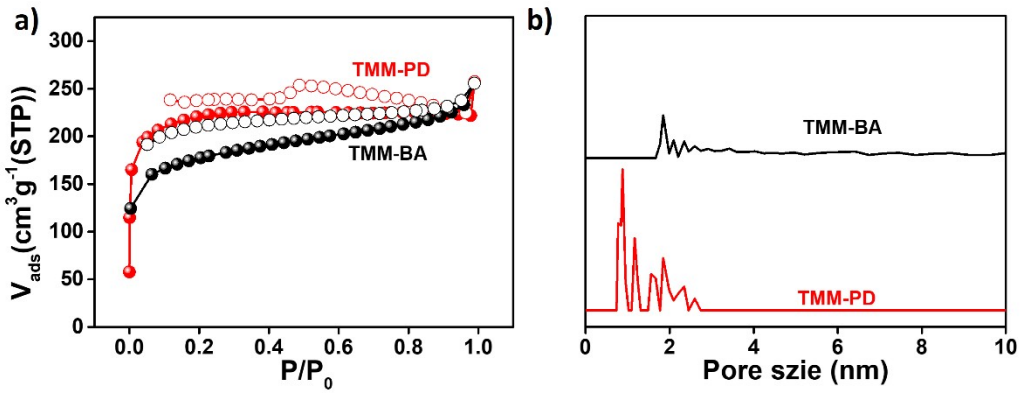

Figure S8. a) N_2 adsorption in TMM-PD and TMM-BA at 77 K. b) Pore size distribution of TMM-PD and TMM-BA.

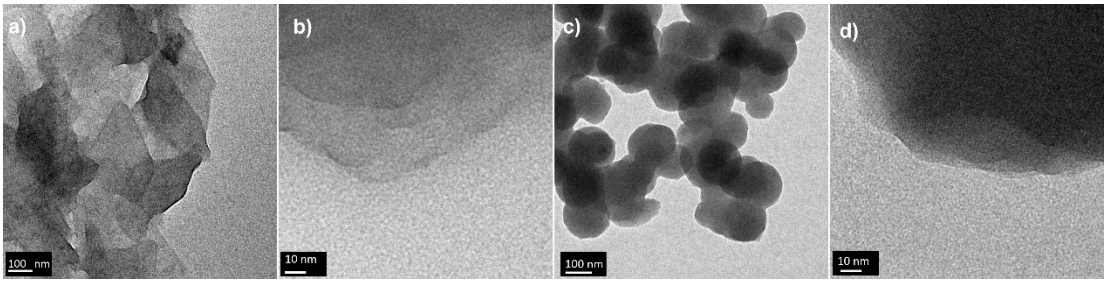

Figure S9. TEM images of a) and b) TMM-PD, c) and d) TMM-BA.

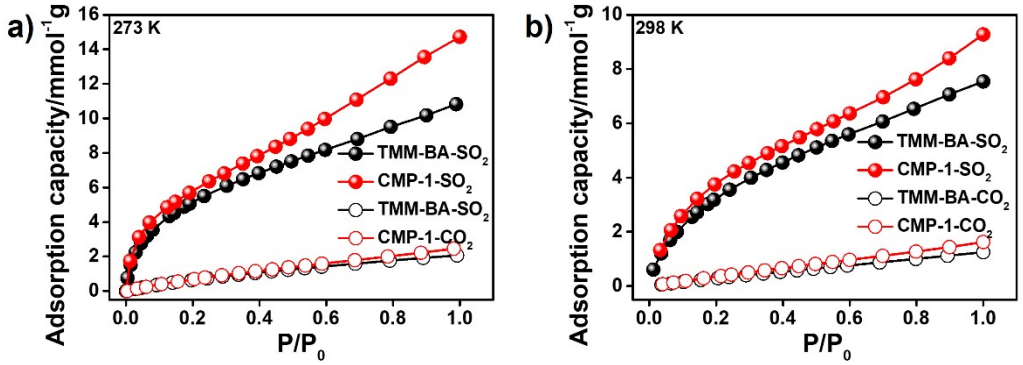

Figure S10. Adsorption capacity of SO_2 and CO_2 in TMM-BA and CMP-1: a) 273 K, b) 298 K.

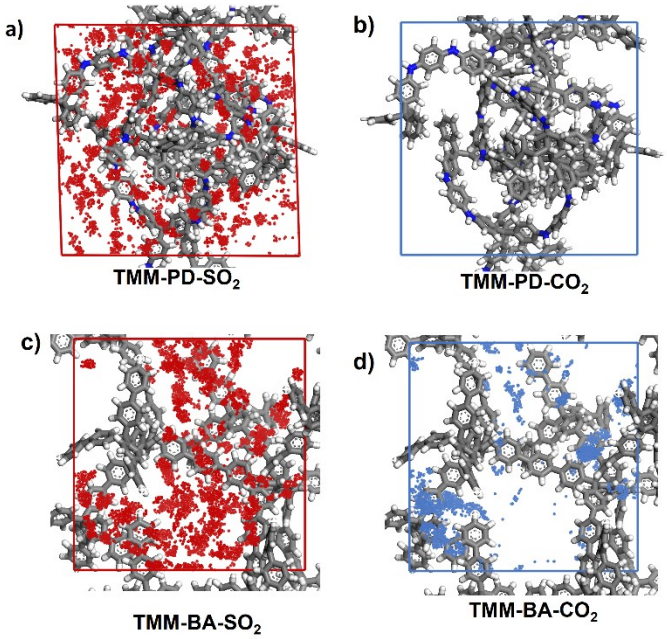

Figure S11. SO_2 adsorption density in a) TMM-PD and c) TMM-BA. CO_2 adsorption density in b) TMM-PD and d) TMM-BA.

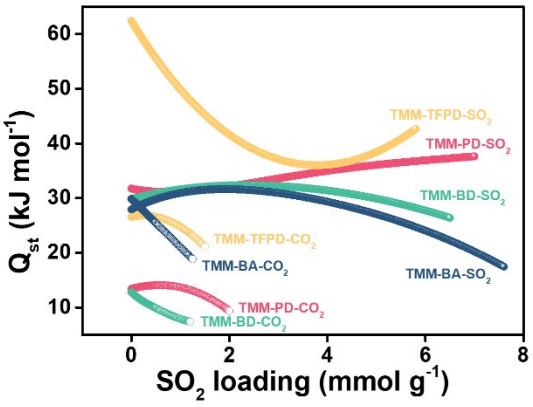

Figure S12. Q_{st} of SO_2 and CO_2 in TMM-PD, TMM-BD, TMM-TFPD, and TMM-BA.

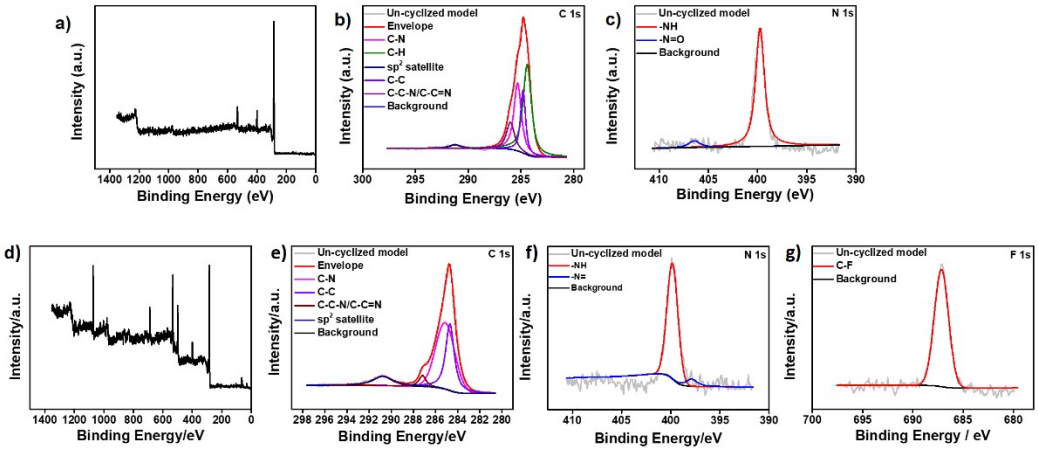

Figure S13. XPS spectra of a)-c) TMM-BD, d)-g) TMM-TFPD.

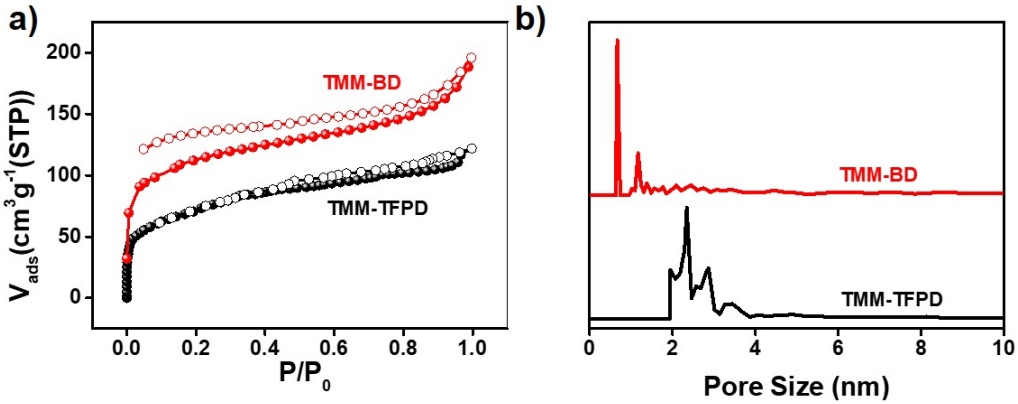

Figure S14. a) N_2 adsorption isotherm of TMM-BD and TMM-TFPD at 77 K. b) Pore size distribution of TMM-BD and TMM-TFPD.

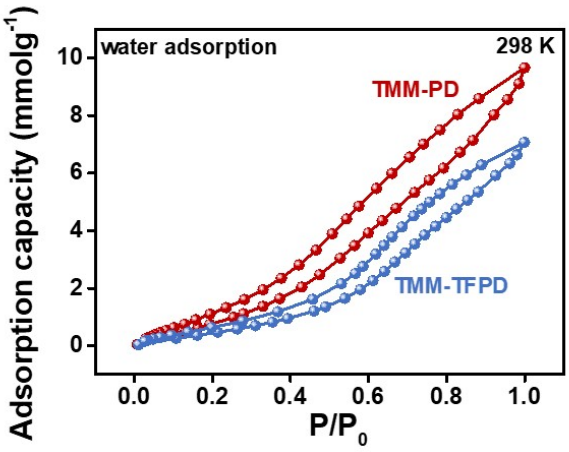

Figure S15. Water Adsorption isotherm of TMM-PD and TMM-TFPD at 298 K.

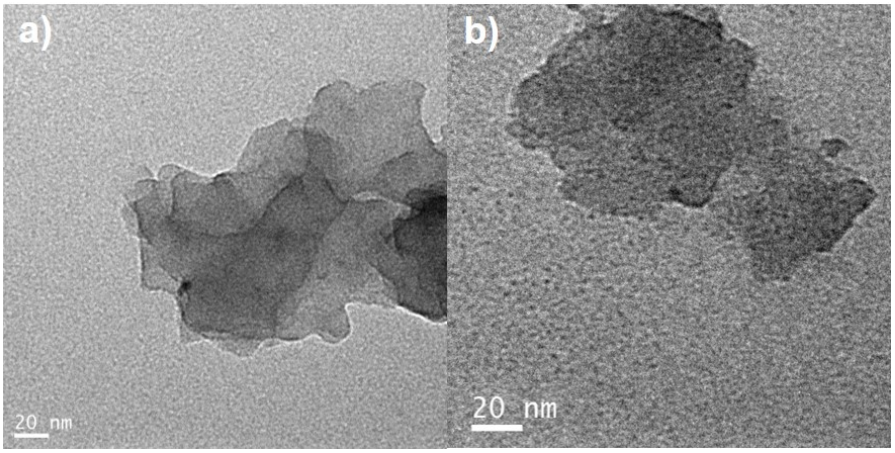

Figure S16. TEM images of a) TMM-BD and b) TMM-TFPD.

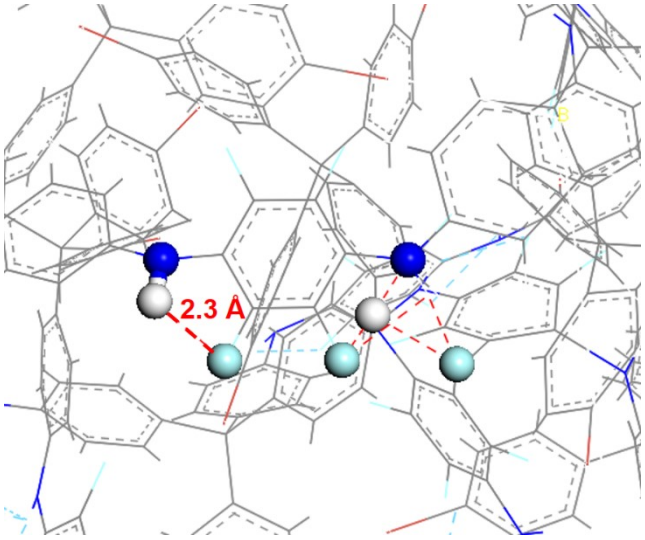

Figure S17. The intramolecular hydrogen bond between imine group and fluorine group in TMM-TFPD.

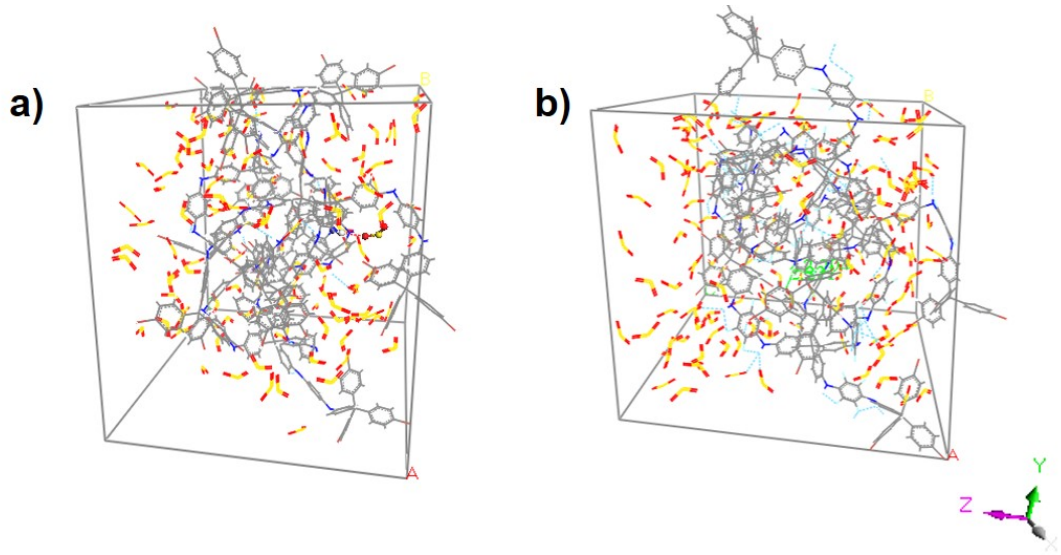

Figure S18. GCMC simulated adsorption of SO_2 in a) TMM-PD and d) TMM-TFPD at 298 K and 1 bar.

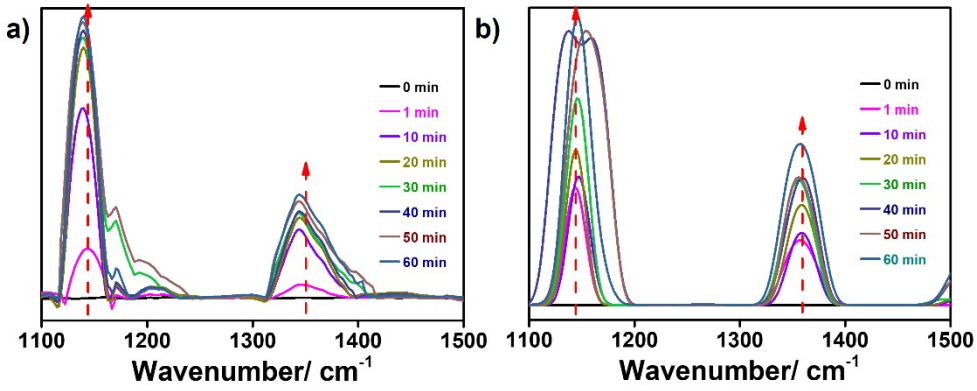

Figure S19. In-situ FTIR spectra of a) TMM-PD and b) TMM-TFPD at various times within 60 mins under 2000 ppm SO_2 at 298 K.

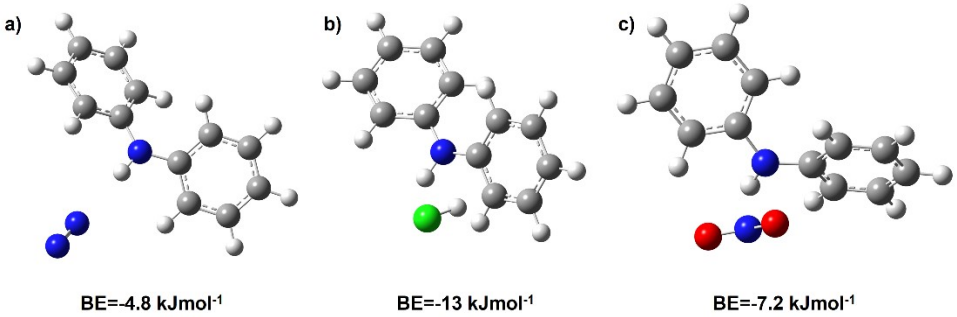

Figure S20. BEs between -NH- linkage with a) N_2, b) HCl, and c) NO_2.

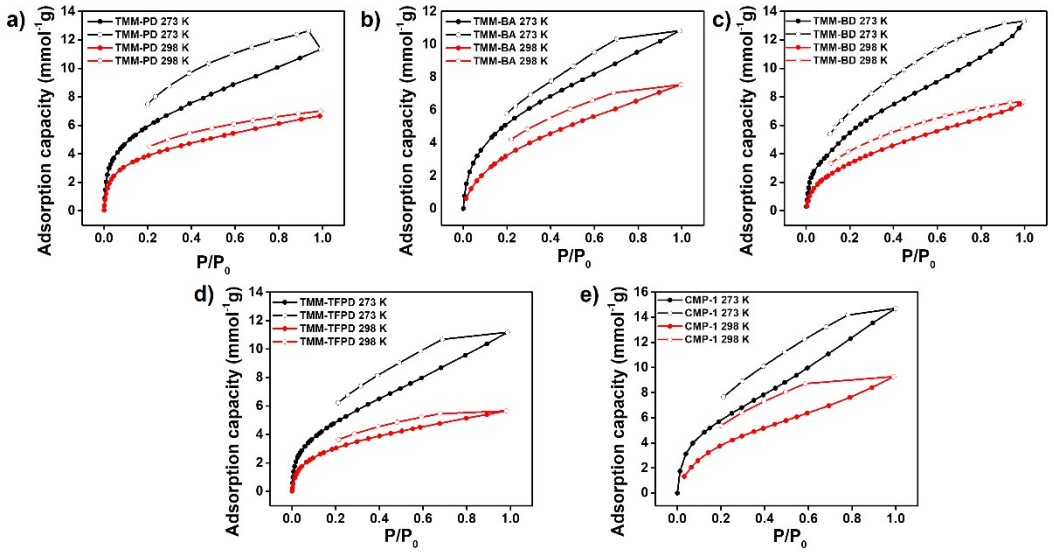

Figure S21. SO_2 adsorption and desorption isotherms of a) TMM-PD, b) TMM-BA, c) TMM-BD, d) TMM-TFPD, and e) CMP-1.

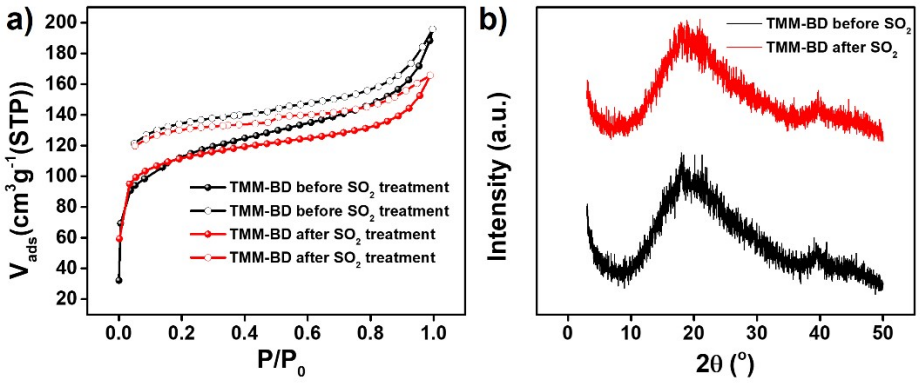

Figure S22. a) N_2 adsorption at 77 K in TMM-BD before and after SO_2 adsorption. B) XRD patterns before and after SO_2 adsorption.

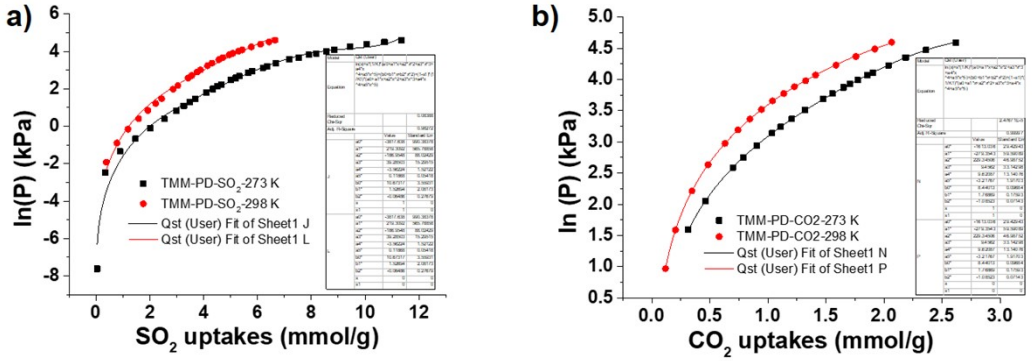

Figure S23. The virial fitting of a) SO_2 and b) CO_2 sorption data in TMM-PD.

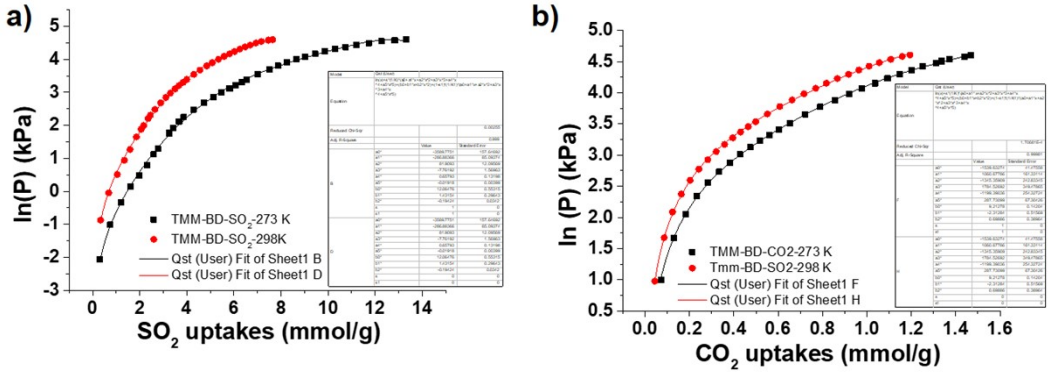

Figure S24. The virial fitting of a) SO_2 and b) CO_2 sorption data in TMM-BD.

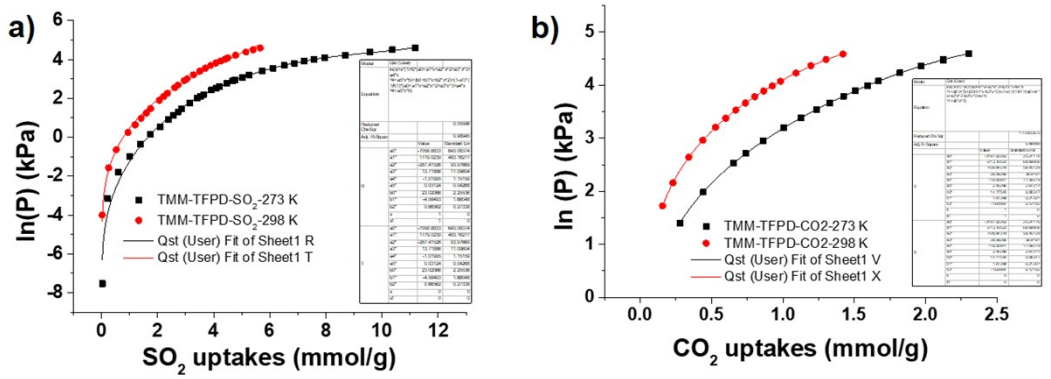

Figure S25. The virial fitting of a) SO_2 and b) CO_2 sorption data in TMM-TFPD.

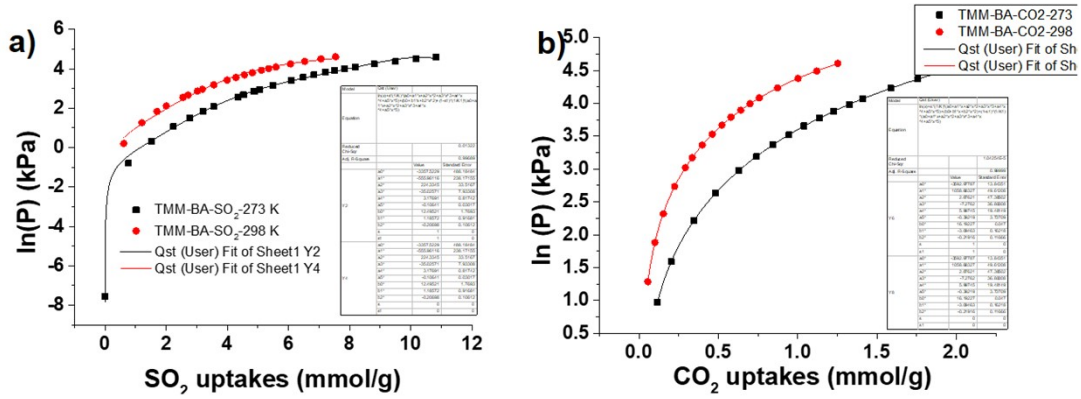

Figure S26. The virial fitting of a) SO_2 and b) CO_2 sorption data in TMM-BA.

Section 4. Supporting Tables

Table S1 Summary of equation parameters of the dual-site Langmuir-Freundlich model for SO_2 and CO_2 at 298 K.

Sample	gas	Parament: a	Parament: k	Parament: b	Parament: y
TMM-PD	SO_2	10.57463	0.00538	2.99408	0.6884
	CO_2	0.4258	0.04276	11936.0342	$1.17552^{x}10^{-6}$
TMM-BD	SO_2	33.01408	0.00182	2.47937	0.3359
	CO_2	0.00434	$-1.90302^{x}10^{31}$	4.33152	0.00367
TMM-TFPD	SO_2	2.35143	0.46384	10.77084	0.00454
	CO_2	4970.81776	$1.82306^{x}10^{-6}$	0.68048	0.03274
TMM-BA	SO_2	48512.39003	$1.26286^{x}10^{-6}$	3.08593	0.19992
	CO_2	-1.92748	$6.70344^{x}10^{-4}$	27.82444	$6.69996^{x}10^{-4}$
CMP-1	SO_2	0.00128	2.6615	2.60842	0.78601
	CO_2	$1.29968^{x}10^{4}$	5.03589	0.10294	0.95796

Table S2 Comparison table relevant to the SO_2/CO_2 separation performance with reported works.

Materials	BET surface area (m^2g^{-1})	SO_2 uptakes ($mmolg^{-1}$)			CO_2 uptakes[a] ($mmolg^{-1}$)	SO_2 elute time ($ming^{-1}$)	References
		0.02 bar	0.1 bar	1 bar			
SIFSIX-1-Cu	-	2.31	8.74	11.01	4.5	800	6
Mn-CUK-1	599	1.2	1.93	5.51	-	-	7
MOF-303	1211	3.7	6.21	7.86	3.35	-	8
[Ir]@NU-1000	1842	0.5	2.4	10.9	-	-	9
$[Pd_6L_8](NO_3)_{36}$	111	-	0.9	6	-	-	10
Zr-Fum	600	1.2[d]	3.1	4.9	1.2[e]	-	
MOF-808	1990	2.1[d]	3.6	14.6	1[e]	-	
DUT-67(Zr)	1260	0.7[d]	2.3	9	0.9[e]	-	
NU-1000	1740	0.6[d]	2.6	12.2	1[e]	-	
MIL-53(Al)	1450	0.4[d]	3.3	10.5	1.4[e]	-	

NH_2-MIL-53(Al)	620	2[d]	4.3	8	2.1[e]	-	
Al-Fum	970	1[d]	4.1	7.5	1.5[e]	-	
MIL-53(tdc)(Al)	1000	0.6[d]	5	6.9	1.4[e]	-	
CAU-10-H	600	1.2[d]	3.7	4.8	1.7[e]	-	
MIL-96(Al)	530	1.2[d]	3.7	6.5	3[e]	-	
MIL-100(Al)	1890	0.4[d]	2.5	16.3	0.8[e]	-	
NH_2-MIL-101(Al)	1770	1.5[d]	3.6	17.3	1.6[e]	-	
MIL-53(Al)-TDC	1260	4.7[f]	-	8.9	3	-	12
MIL-53(Al)-BDC	1210	0.6[f]	-	10.8	2	-	
$[Zn_2(L1)_2(bipy)]$	47	-	-	10.9	1.15	-	13
CC3	-	-	-	2.78	-	-	5
RCC3	-	-	-	12.34	-	-	
6FT-RCC3	396	3.57[d]	8.67	13.78	-	-	
DMOF	1956	0.25[d]	7.21	13.09		28	14
DMOF-M	1557	0.46[d]	6.4	12.15			
DMOF-DM	1343	1[d]	5.7	10.4			
DMOF-TM	900	3.79[d]	6.43	9.68		346	
MIL-160		4.2[d]	5.5	7.2	-	600[g]	15
MFM-422	3296	-	6.2	7.8	2.5	200	16
MFM-305-CH_3	256	3.59	-	5.16	2.41	-	17
MFM-305	779	3.94	-	6.99	3.02	500	
MIL-101(Cr)-4F(1%)	2176	-	4.5	18.4	-	-	18
CAU-10	630	-	3.9	4.47	-	-	19
NanoCB6–H	441	-	-	4.98	2.6	-	20
Mg_2(dobpdc)	3300	6[f]	-	19.5	6	-	21

MFM-101	2300	-	-	18.7	-	230	22
MFM-190(F)	2538	-	-	18.3	-	190	
MFM-601	3644	-	-	12.3	1.3	30	23
P(Ph-4MVIm-Br)	285	1.55	4.14	8.12	0.67	1200	3
KAUST-8	258	0.2	1.6	-	-	500	24
P(3DVB-[VEIm]Br)	382			7.7	-70	70	25
MFM-300(Cr)	1360	-	-	10[c]	7.37	76	26
MFM-170	2408	6.5[c]	-	17.5	3.04	33[b]	27
ECUT-111	1493	1.8	6.4	11.6	3.3	180	28
ECUT-100	688	1.88	3.3	4.95	2.76	151	29
Cage-U-Co-MOF	208	0.75	1.25	3.5	0.75	152	30
TMM-BD	435	-	2.5	7.65	1.1	185	This work
TMM-PD	6.2	-	3.2	6.65	1.3	180	This work
TMM-TFPD	254	-	2.35	5.65	1	122	This work

[a] 1 bar, [b] 323 K, [c]273 K, [d] 0.01 bar, [e] 0.5 bar, [f] 0.05 bar, [g] 10000 ppm and 293 K.

Section 5. References

1. L. Sun, Y. Zou, Z. Liang, J. Yu and R. Xu, *Polym. Chem.*, 2014, **5**, 471-478.
2. J. X. Jiang, F. Su, A. Trewin, C. D. Wood, N. L. Campbell, H. Niu, C. Dickinson, A. Y. Ganin, M. J. Rosseinsky, Y. Z. Khimyak and A. I. Cooper, *Angewandte Chemie*, 2007, **46**, 8574-8578.
3. X. Suo, Y. Yu, S. Qian, L. Zhou, X. Cui and H. Xing, *Angewandte Chemie*, 2021, **133**, 7062-7067.
4. F. Chen, D. Lai, L. Guo, J. Wang, P. Zhang, K. Wu, Z. Zhang, Q. Yang, Y. Yang, B. Chen, Q. Ren and Z. Bao, *Journal of the American Chemical Society*, 2021, **143**, 9040-9047.
5. I. Ibarra, E. Martínez-Ahumada, D. He, V. Berryman, V. Jancik, V. Martis, M. A. Vera, E. Lima, D. J. Parker and A. I. Cooper, *Angewandte Chemie International Edition*, 2021.
6. X. Cui, Q. Yang, L. Yang, R. Krishna, Z. Zhang, Z. Bao, H. Wu, Q. Ren, W. Zhou, B. Chen and H. Xing, *Advanced materials*, 2017, **29**.
7. S. G. Dunning, N. K. Gupta, J. E. Reynolds, 3rd, M. Sagastuy-Brena, J. G. Flores, E. Martinez-Ahumada, E. Sanchez-Gonzalez, V. M. Lynch, A. Gutierrez-Alejandre, J. Aguilar-Pliego, K. S. Kim, I. A. Ibarra and S. M. Humphrey, *Inorganic chemistry*, 2022, **61**, 15037-15044.
8. J. L. Obeso, E. Martínez-Ahumada, A. López-Olvera, J. Ortiz-Landeros, H. A. Lara-García, J. Balmaseda, S. López-Morales, E. Sánchez-González, D. Solis-Ibarra, C. Leyva and I. A. Ibarra, *ACS Applied Energy Materials*, 2022, DOI: 10.1021/acsaem.2c02983.
9. S. Gorla, M. L. Diaz-Ramirez, N. S. Abeynayake, D. M. Kaphan, D. R. Williams, V. Martis, H. A. Lara-Garcia, B. Donnadieu, N. Lopez, I. A. Ibarra and V. Montiel-Palma, *ACS applied materials & interfaces*, 2020, **12**, 41758-41764.
10. S. J. Valencia-Loza, A. Lopez-Olvera, E. Martinez-Ahumada, D. Martinez-Otero, I. A. Ibarra, V. Jancik and E. G. Percastegui, *ACS applied materials & interfaces*, 2021, **13**, 18658-18665.
11. P. Brandt, S. H. Xing, J. Liang, G. Kurt, A. Nuhnen, O. Weingart and C. Janiak, *ACS applied materials & interfaces*, 2021, **13**, 29137-29149.
12. A. Lopez-Olvera, J. A. Zarate, E. Martinez-Ahumada, D. Fan, M. L. Diaz-Ramirez, P. A. Saenz-Cavazos, V. Martis, D. R. Williams, E. Sanchez-Gonzalez, G. Maurin and I. A. Ibarra, *ACS applied materials & interfaces*, 2021, **13**, 39363-39370.
13. S. Glomb, D. Woschko, G. Makhloufi and C. Janiak, *ACS applied materials & interfaces*, 2017, **9**, 37419-37434.
14. S. Xing, J. Liang, P. Brandt, F. Schafer, A. Nuhnen, T. Heinen, I. Boldog, J. Mollmer, M. Lange, O. Weingart and C. Janiak, *Angewandte Chemie*, 2021, **60**, 17998-18005.
15. P. Brandt, A. Nuhnen, M. Lange, J. Mollmer, O. Weingart and C. Janiak, *ACS applied materials & interfaces*, 2019, **11**, 17350-17358.
16. J. Li, G. L. Smith, Y. Chen, Y. Ma, M. Kippax-Jones, M. Fan, W. Lu, M. D. Frogley, G. Cinque, S. J. Day, S. P. Thompson, Y. Cheng, L. L. Daemen, A. J. Ramirez-Cuesta, M. Schroder and S. Yang, *Angewandte Chemie*, 2022, **61**, e202207259.
17. L. Li, I. da Silva, D. I. Kolokolov, X. Han, J. Li, G. Smith, Y. Cheng, L. L. Daemen, C. G. Morris, H. G. W. Godfrey, N. M. Jacques, X. Zhang, P. Manuel, M. D. Frogley, C. A. Murray, A. J. Ramirez-Cuesta, G. Cinque, C. C. Tang, A. G. Stepanov, S. Yang and M. Schroder, *Chemical science*, 2019, **10**, 1472-1482.
18. E. Martínez-Ahumada, M. L. Díaz-Ramírez, H. A. Lara-García, D. R. Williams, V. Martis, V. Jancik, E. Lima and I. A. Ibarra, *Journal of Materials Chemistry A*, 2020, **8**, 11515-11520.
19. J. A. Zarate, E. Dominguez-Ojeda, E. Sanchez-Gonzalez, E. Martinez-Ahumada, V. B. Lopez-Cervantes, D. R. Williams, V. Martis, I. A. Ibarra and J. Alejandre, *Dalton Trans*, 2020, **49**, 9203-9207.
20. J. Liang, S. Xing, P. Brandt, A. Nuhnen, C. Schlüsener, Y. Sun and C. Janiak, *Journal of Materials Chemistry A*, 2020, **8**, 19799-19804.
21. E. Martínez-Ahumada, D. w. Kim, M. Wahiduzzaman, P. Carmona-Monroy, A. López-Olvera, D. R. Williams, V. Martis, H. A. Lara-García, S. López-Morales, D. Solis-Ibarra, G. Maurin, I. A. Ibarra and C. S. Hong, *Journal of Materials Chemistry A*, 2022, **10**, 18636-18643.
22. W. Li, J. Li, T. D. Duong, S. A. Sapchenko, X. Han, J. D. Humby, G. F. S. Whitehead, I. J. Victorica-Yrezabal, I. da Silva, P. Manuel, M. D. Frogley, G. Cinque, M. Schroder and S. Yang, *Journal of the American Chemical Society*, 2022, **144**, 13196-13204.
23. J. H. Carter, X. Han, F. Y. Moreau, I. da Silva, A. Nevin, H. G. W. Godfrey, C. C. Tang, S. Yang and M. Schroder, *Journal of the American Chemical Society*, 2018, **140**, 15564-15567.
24. M. R. Tchalala, P. M. Bhatt, K. N. Chappanda, S. R. Tavares, K. Adil, Y. Belmabkhout, A. Shkurenko, A. Cadiau, N. Heymans, G. De Weireld, G. Maurin, K. N. Salama and M. Eddaoudi, *Nature communications*, 2019, **10**, 1328.
25. L. Xia, Q. Cui, X. Suo, Y. Li, X. Cui, Q. Yang, J. Xu, Y. Yang and H. Xing, *Advanced Functional Materials*, 2018, **28**, 1704292.
26. L. Briggs, R. Newby, X. Han, C. G. Morris, M. Savage, C. P. Krap, T. L. Easun, M. D. Frogley, G. Cinque, C. A. Murray, C. C. Tang, J. Sun, S. Yang and M. Schröder, *Journal of Materials Chemistry A*, 2021, **9**, 7190-7197.
27. G. L. Smith, J. E. Eyley, X. Han, X. Zhang, J. Li, N. M. Jacques, H. G. W. Godfrey, S. P. Argent, L. J. McCormick McPherson, S. J. Teat, Y. Cheng, M. D. Frogley, G. Cinque, S. J. Day, C. C. Tang, T. L. Easun, S. Rudic, A. J. Ramirez-Cuesta, S. Yang and M. Schroder, *Nature materials*, 2019, **18**, 1358-1365.
28. M. J. Yin, X. H. Xiong, X. F. Feng, W. Y. Xu, R. Krishna and F. Luo, *Inorganic chemistry*, 2021, **60**, 3447-3451.
29. L. J. Guo, X. F. Feng, Z. Gao, R. Krishna and F. Luo, *Inorganic chemistry*, 2021, **60**, 1310-1314.
30. Y. Fan, M. Yin, R. Krishna, X. Feng and F. Luo, *Journal of Materials Chemistry A*, 2021, **9**, 4075-4081.
31. M. J. Frisch, G. W. Trucks, H. B. Schlegel, G. E. Scuseria, M. A. Robb, J. R. Cheeseman, G. Scalmani, V. Barone, B. Mennucci, G. A. Petersson, H. Nakatsuji, M. Caricato, X. Li, H. P. Hratchian, A. F. Izmaylov, J. Bloino, G. Zheng, J. L. Sonnenberg, M. Hada, M. Ehara, K. Toyota, R. Fukuda, J. Hasegawa, M. Ishida, T. Nakajima, Y. Honda, O. Kitao, H. Nakai, T. Vreven, J. A. Montgomery Jr., J. E. Peralta, F. Ogliaro, M. Bearpark, J. J. Heyd, E. Brothers, K.

N. Kudin, V. N. Staroverov, T. Keith, R. Kobayashi, J. Normand, K. Raghavachari, A. Rendell, J. C. Burant, S. S. Iyengar, J. Tomasi, M. Cossi, N. Rega, J. M. Millam, M. Klene, J. E. Knox, J. B. Cross, V. Bakken, C. Adamo, J. Jaramillo, R. Gomperts, R. E. Stratmann, O. Yazyev, A. J. Austin, R. Cammi, C. Pomelli, J. W. Ochterski, R. L. Martin, K. Morokuma, V. G. Zakrzewski, G. A. Voth, P. Salvador, J. J. Dannenberg, S. Dapprich, A. D. Daniels, O. Farkas, J. B. Foresman, J. V. Ortiz, J. Cioslowski, D. J. Fox, Gaussian 09, Revision D.01, Gaussian, Inc., Wallingford, CT 2013.

32. J. Andzelm, R. King-Smith and G. Fitzgerald, *Chemical physics letters*, 2001, 335, 321-326.